Long-range surface plasmon-polariton waveguide sensors with a Bragg grating in the asymmetric double-electrode structure

Yang Hyun Joo,[1] Seok Ho Song,[1,*] and Robert Magnusson[2]

[1]Department of Physics, University of Hanyang, Seoul 133-790, Korea
[2]*Department of Electrical Engineering, University of Texas at Arlington, USA*
**shsong@hanyang.ac.kr*

Abstract: We propose a Bragg grating resonance sensor based on long-range surface plasmon-polaritons (LRSPP) excited on an asymmetric double-electrode waveguide structure. The proposed LRSPP waveguide sensor utilizes spectral resonance of the asymmetric double-electrode structure by adding a Bragg grating layer on the top surface of the metal slab. We have numerically estimated the bulk index resolution and thickness detection limit of a target biomolecule layer under 30 dB total propagation loss. The sub-μm fluidic channel between the two metal layers always experiences a highly confined LRSPP mode excited by end-fire coupling with optical fibers, therefore the proposed LRSPP sensor platform can be applied to a variety of integrated sensor-chip scenarios.

OCIS codes: (204.6680) Surface plasmons; (130.6010) Sensors; (230.7370) Waveguides.

References and links

1. X. D. Hoa, A. G. Kirk, and M. Tabrizian, "Towards integrated and sensitive surface plasmon resonance biosensors: a review of recent progress," Biosens. Bioelectron. **23**(2), 151–160 (2007).
2. J. Homola, "Surface plasmon resonance sensors for detection of chemical and biological species," Chem. Rev. **108**(2), 462–493 (2008).
3. P. Berini, "Bulk and surface sensitivities of surface plasmon waveguides," N. J. Phys. **10**(10), 105010 (2008).
4. Website, http://www.biacore.com/lifesciences/index.html.
5. X. Fan, I. M. White, S. I. Shopova, H. Zhu, J. D. Suter, and Y. Sun, "Sensitive optical biosensors for unlabeled targets: a review," Anal. Chim. Acta **620**(1-2), 8–26 (2008).
6. J. Homola, S. S. Yee, and G. Gauglitz, "Surface plasmon resonance sensors: review," Sens. Actuators B Chem. **54**(1-2), 3–15 (1999).
7. G. Nemova, and R. Kashyap, "Fiber-Bragg-grating-assisted surface plasmon-polariton sensor," Opt. Lett. **31**(14), 2118–2120 (2006).
8. M.-H. Chiu, S.-F. Wang, and R.-S. Chang, "D-type fiber biosensor based on surface-plasmon resonance technology and heterodyne interferometry," Opt. Lett. **30**(3), 233–235 (2005).
9. S. M. Tripathi, A. Kumar, E. Marin, and J.-P. Meunier, "Side-polished optical fiber grating-based refractive index sensors utilizing the pure surface plasmon polariton," J. Lightwave Technol. **26**(13), 1980–1985 (2008).
10. G. G. Nenninger, P. Tobiska, J. Homola, and S. S. Yee, "Long-range surface plasmons for high-resolution surface plasmon resonance sensors," Sens. Actuators B Chem. **74**(1-3), 145–151 (2001).
11. P. Berini, R. Charbonneau, and N. Lahoud, "Long-range surface plasmons on ultrathin membranes," Nano Lett. **7**(5), 1376–1380 (2007).
12. Y. H. Joo, M. J. Jung, J. Yoon, S. H. Song, H. S. Won, S. Park, and J. J. Ju, "Long-range surface plasmon polaritons on asymmetric double-electrode structures," Appl. Phys. Lett. **92**(16), 161103 (2008).
13. E. N. Economou, "Surface plasmons in thin films," Phys. Rev. **182**(2), 539–554 (1969).
14. We used a commercial FEM tool of FEMLAB™ 3.1 (now, MULTIPHYSICS™), COMSOL, Inc.
15. C. M. Kim, and R. V. Ramaswamy, "Overlap integral factors in integrated optic modulators and switches," J. Lightwave Technol. **7**(7), 1063–1070 (1989).
16. P. Yeh, *Optical waves in layered Media* (Wiley and Sons, New York, 1988).

#111165 - $15.00 USD Received 11 May 2009; revised 3 Jun 2009; accepted 3 Jun 2009; published 9 Jun 2009

1. Introduction

Surface plasmon resonance (SPR) sensors have been extensively explored as being among the foremost sensor types for label-free observation of interactions between target analytes and biorecognition molecules [1–3]. Commercialized SPR sensors which are typically based on prism coupling have a refractive index resolution between 10^{-7} and 10^{-6} refractive-index units (RIU) [4]. Prism coupling is the most convenient and sensitive configuration among the SPR platforms [5,6], but the prism is too bulky to integrate. Another possible method for exciting the SPR is waveguide coupling which is robust and easy to integrate with other components. Metal-clad leaky waveguide structures that utilize short-range surface plasmon polaritons (SPP) excited on a metal layer deposited on a dielectric waveguide or a side-polished single mode fiber usually have resolution from10^{-6} to 10^{-5} RIU [7–9].

To improve the resolution and reduce the high attenuation of waveguide-based SPR biosensors, it is desirable to use a long-range SPP (LRSPP) which consists of coupled surface plasma waves existing on opposite sides of a thin metal film suspended between two dielectrics [10]. The longer propagation length of LRSPP reduces the resonance width and increases the sensitivity of the sensor, but the requirement that the two dielectrics embedding the thin metal film must be identical is very strict. The constraints imposed by the symmetry requirement of LRSPP waveguide sensors can be circumvented by using a large-area, ultrathin dielectric membrane upon which a thin metal film or a metal stripe pattern is deposited, and allowing the gaseous or liquid environment to surround the structure [11]. The introduction of a thin membrane can also enhance the LRSPP field amplitude localized to the top metal surface for superior sensitivity, but the construction of a ~20 nm-thin, metal-on-membrane bridge in a sensor structure is still challenging from practical points of view.

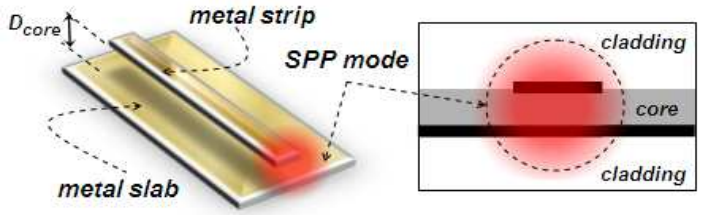

Fig. 1. Schematic of an asymmetric double-electrode LRSPP waveguide.

Recently we proposed an asymmetric double-electrode LRSPP waveguide structure with a finite width metal strip on top of a thin metal slab and with a core dielectric (thickness, D_{core}) between the metal layers. A conceptual scheme of LRSPP guiding on the asymmetric double-electrodes is depicted in Fig. 1 [12]. The LRSPP mode propagating along the asymmetric electrodes are laterally confined by the ~5 μm-wide metal strip and the lower metal slab; therefore, the mode profile becomes almost circularly symmetric as depicted by a dashed circle in Fig. 1. Propagation losses of the mode and efficiency in coupling to single-mode fibers at telecom wavelengths are comparable to those of single-stripe LRSPP waveguides. Note that, while maintaining the symmetry between the top and bottom claddings, the central thin slab of the dielectric core bounded by the two metal layers can be filled with a different dielectric, or even with gaseous and aqueous biomolecules. That means that the core layer can act as a micro-fluidic channel in a sensor chip. Several waveguide structures, including straight line, S-bend, and Y-branch, were also demonstrated and therefore such an asymmetric double-electrode LRSPP waveguide structure is ready for application to LRSPP waveguide sensors. The geometry in Fig. 1 must be distinguished from the waveguide structure used in the symmetrical metal-clad LRSPP sensors proposed by Economou on which ultrahigh-order modes were excited through free space coupling [13].

Here we design a waveguide-coupling LRSPP biosensor admitting various gaseous or liquid bio/chemical molecules through a μ-fluidic channel. The proposed LRSPP sensor

#111165 - $15.00 USD Received 11 May 2009; revised 3 Jun 2009; accepted 3 Jun 2009; published 9 Jun 2009

utilizes the spectral resonance of the asymmetric double-electrode structure by adding a Bragg grating layer on the top surface of the metal slab. We have estimated the RIU resolution of bulk solution and the detection limit of a binding molecule thickness immobilized on the metal surfaces, while keeping the propagation loss of the asymmetric double-electrode waveguide under a total of 30 dB. Both the RIU resolution on the order of 10^{-6} and the detection thickness limit less than 1 nm strongly depend on the length and modulation depth of the Bragg grating, but they are consistently comparable to the metal-clad leaky waveguide sensors. The sub-μm fluidic channel between the two sensitive metal-layers always experiences a highly confined LRSPP mode excited by end-fire coupling with optical fiber; therefore, the proposed LRSPP sensor platform can be utilized to various integrated sensor applications.

2. Experimental result of a double-electrode waveguide sensor with a μ-fluidic channel

Figure 2(a) shows an asymmetric double-electrode LRSPP waveguide structure with a μ-fluidic channel in the core layer. By completely removing a central part of the core material between the two metal layers, an air channel for passing biomolecule fluid can be formed. Figures 2(b) and 2(c) show the SEM images of the middle and edge of the air channel fabricated by a process similar to that used in Ref. 12. However, in the process used in the figure, an additional layer of a photoresist (PR; AZ5206E, Hoechst High Chem.) was added as sacrificed layer for making the air channel. A 15 μm thick, UV-curable fluorinated resin (ZPU12-470 thermo-optic polymer, ChemOptics Co., n_{clad} = 1.47 at 1550 nm wavelength) was used for the cladding dielectrics and another thermo-optic polymer (ZPU12-450, ChemOptics Co., n_{core} = 1.45) for the 450 nm-thick air channel clearly opened between the cladding layers after removing the PR layer by using a PR developer (AZ340MIF, Hoechst High Chem.) as shown in Fig. 2(b), while the channel edge facing the core layer shown in Fig. 2(c) is not rectangular but tapered. Tapered closing of the channel edges might result from residual PR material. The 5 μm-width metal strip and metal slab layers are not seen in the SEM images because the thickness of the gold layers is just 20 nm. We can evaluate the cut-off core thickness ($D_{cut\text{-}off}$) of the asymmetric LRSPP waveguide structure in terms the core index, n_{core}, by a full vectorial finite-element method (FEM) [14]. For example, $D_{cut\text{-}off}$ = 880 nm when n_{core} = 1.45, and $D_{cut\text{-}off}$ = 130 nm when n_{core} = 1.36. In the fabricated sample with the 450 nm-thick core layer, the fluid inserted into the air channel must have a refractive index greater than 1.43 to keep the LRSPP mode confined.

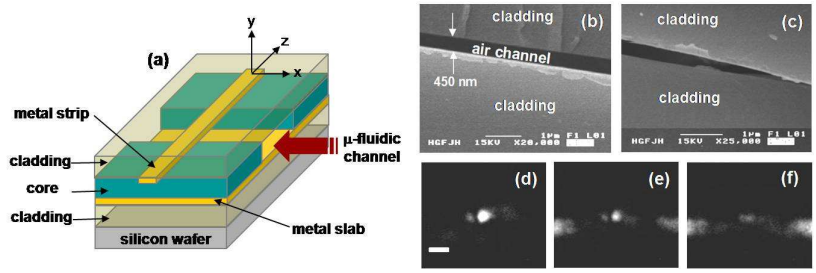

Fig. 2. (a); Schematic of an asymmetric double-electrode LRSPP waveguide structure with a μ-fluidic channel in the core layer. (b) and (c); SEM images of the central and edge parts of the 450 nm-thick, empty μ-fluidic channel. (d)-(f); Far-field output images showing extinction of the LRSPP mode on diluting of the index-matching oil filling the channel with low-index solvent (acetone). The white bar inserted in (d) is 10 μm in length.

LR-SPP modes on the fabricated double-electrode waveguide with a μ-fluidic channel were observed using a fiber-to-waveguide butt coupler consisting of a 1550 nm laser diode (8164A, Agilent Technologies Inc.), a polarization-maintaining single-mode fiber with a lensed facet, a six-axis (three translations and three tilts) stage with a vacuum sample holder, and a far-field microscope with an IR camera. The microscope images of the far-field mode

#111165 - $15.00 USD Received 11 May 2009; revised 3 Jun 2009; accepted 3 Jun 2009; published 9 Jun 2009

profiles after the air channel was filled with a liquid by capillary force are shown in Figs. 2(d)-2(f). When the liquid was an oil (n = 1.45) index-matching with the core dielectric, a circular-symmetric LRSPP mode was clearly measured at the center of the image in Fig. 2(d). The hazy noises around the 8 μm-size mode pattern might be caused by the scattering of the guiding mode mostly at the tapered boundaries of the channel edges shown in Fig. 2(c). If we dropped a solvent of acetone (n = 1.36) near the channel entrance which was already filled with the index matching oil, the high-index oil was dissolved out of the channel and then the refractive index of the composite liquid inside the channel fell gradually down to the acetone index of 1.36. Note that $D_{cut\text{-}off}$ = 130 nm when n_{core} = 1.36, therefore the far-field output images in Figs. 2(e) and 2(f) reveal extinction of the LRSPP mode as the index-matching oil is diluted with the low-index solvent (acetone). We could see the mode image shown in Fig. 2(d) again after a few minutes since the channel was refilled with the oil as soon as the acetone solvent was volatilized out of the channel region. Reappearance of the mode reveals that the metal and dielectric layers surrounding the channel endure the acetone infiltration. Therefore we conclude that the mode disappearance in Figs. 2(e) and 2(f) must originate in the index difference and associated mode cut-off.

Such a variation characteristic in mode size or mode energy according to the change in refractive index of the channel fluid allows the asymmetric waveguide structure to be eligible for a sensor chip. However, the slope of mode variation in size or energy is so slow even near the mode cut-off boundaries that it may not be acceptable for a good refractometer with RIU resolution less than 10^{-6}. To enhance the sensing resolution of the asymmetric double-electrode waveguide structure, we add on the metal-slab a Bragg grating with a period of Λ as shown in Fig. 3.

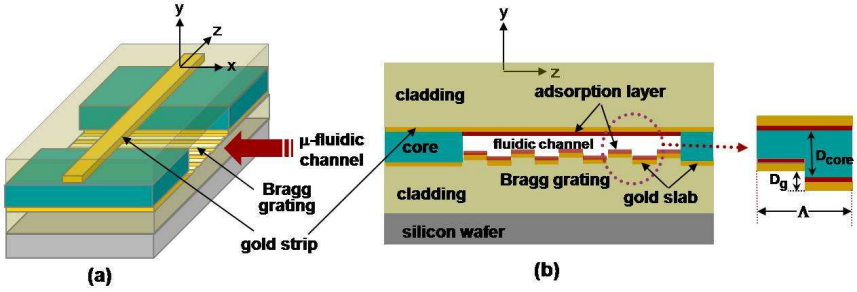

Fig. 3. Schematics of the asymmetric double-electrode LRSPP biosensor. A Bragg grating on the bottom of the channel is shown in (a). Details including the biorecognition layers covering the gold strip and slab surfaces are in (b), and a single period (Λ) of the Bragg grating with a height of D_g in (c)

3. Numerical result of the proposed LR-SPP sensor

For the core material we assumed Cytop (Asahi Glass Co.), an amorphous fluoropolymer closely index matched to water (n = 1.33), MgF_2 (n = 1.35) for the cladding, gold layer thickness of 20 nm, gold strip width of 5 μm, and a core thickness D_{core} of 450 nm. D_g is the modulation depth of half of one period. Adsorption layers (n = 1.5) of biorecognition molecules, such as antibodies, are immobilized on both metal surfaces facing the fluidic channel as depicted in Fig. 3(b). Initially, the μ-fluidic channel is filled with a buffer solution of water. The binding of target biomolecules (n = 1.5) to the adsorption layers results in a refractive-index change near the metal surfaces, which can be detected as a sensing transduction signal by monitoring the shift in the peak wavelength of resonant reflectance or transmittance of the guided LRSPP modes. The resonance wavelength of the Bragg gratings is given by $\lambda_B = 2\Lambda \cdot n_{eff}$, where n_{eff} is the effective index of the LR-SPP mode supported by the asymmetric waveguide with the Bragg grating structure. The n_{eff} can be determined numerically by averaging two LRSPP mode indices for the core thickness of D_{core} and D_{core} -

#111165 - $15.00 USD Received 11 May 2009; revised 3 Jun 2009; accepted 3 Jun 2009; published 9 Jun 2009

D_g [14]. For D_{core} = 450 nm and D_g = 60 nm, n_{eff} ~1.351, therefore Λ ~575 nm at λ_B = 1553.5 nm.

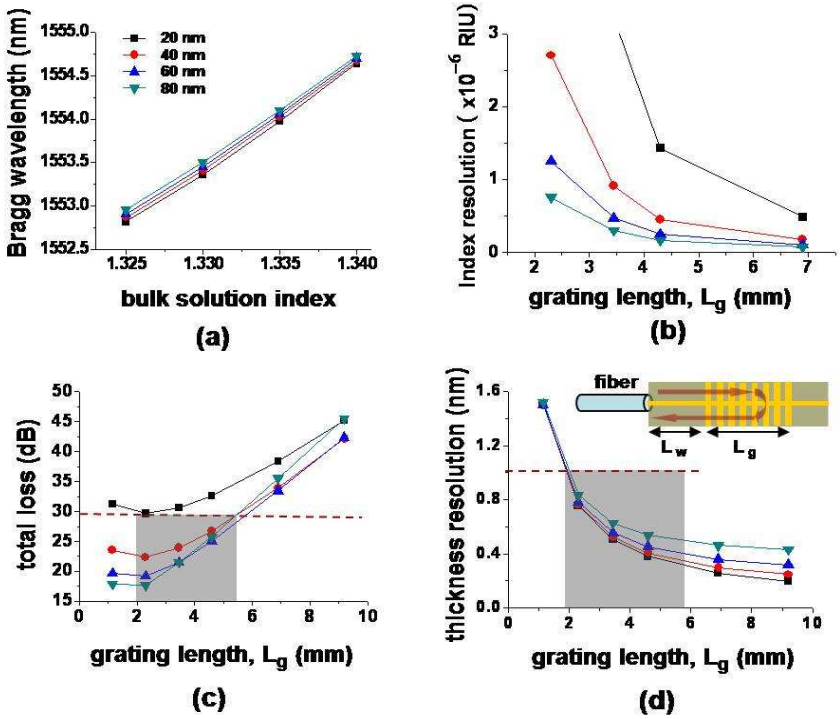

Fig. 4. Numerical estimation of index and thickness resolutions of the asymmetric LRSPP waveguide sensor. Measurement setup is depicted in the inset of (d), and four different grating heights, D_g, from 20 nm to 80 nm, are considered and are denoted by four different symbols in (a). (a) Bragg wavelength shift with different refractive index of the bulk solution filling the fluidic channel. (b) Refractive index resolution with various grating lengths, L_g, defined in the inset of (d). (c) Total loss of the fiber butt-coupled asymmetric waveguide sensor. (d) Thickness resolution of the biomolecular adsorption layer.

Estimation results for sensing resolutions of the asymmetric LRSPP waveguide sensor in terms of the fluid index and the adsorption layer thickness are presented in Fig. 4. Here, we consider a measurement setup as depicted in the inset of Fig. 4(d), where the LRSPP waveguide is butt-coupled to a single-mode optical fiber for signal input and output at the 1550-nm telecomm wavelength. The length of the μ-fluidic channel embedding the Bragg grating is L_g, and the gap distance between the fiber and the grating is L_w. Four different grating heights, D_g, from 20 nm to 80 nm, are considered and are denoted by four different symbols in Fig. 4(a). Figure 4(a) shows the Bragg wavelength shift when the refractive index of the bulk solution filled in the fluidic channel is varied from 1.325 to 1.340. Regardless of the grating depth, the slopes of the wavelength shift in bulk index variation are nearly constant, about ~120 nm/RIU. If we can detect a 1.0 pm shift in the wavelength peak, which is about 1% of the full-width at half maximum (FWHM) of the reflection signal [7,9], the bulk index resolution of the asymmetric LRSPP waveguide sensor is of the order of 10^{-7} ~10^{-6} RIU, as shown in Fig. 4(b). Longer and shallower gratings provide higher sensitivity in index change. With a 10% FWHM detection limit, ~10^{-6} RIU resolution can be achieved with a 20 nm height grating structure.

Figure 4(c) shows the total optical loss of the measurement setup defined by $\eta_{total} = (\eta_{fiber}\eta_w\eta_g)^2 R_{Bragg}$, where η_{fiber} is the coupling loss to fiber, η_W and η_g are the

#111165 - $15.00 USD Received 11 May 2009; revised 3 Jun 2009; accepted 3 Jun 2009; published 9 Jun 2009

propagation losses of LRSPP mode on the L_w (= 1 mm) waveguide-only area and the L_g (1 mm ~10 mm) grating area, and R_{Bragg} the reflectance of Bragg grating. The square factor in the total loss is due to the round trip of the optical signal. We used the mode overlap integral method in η_{fiber} calculation of a single-mode fiber coupling to the 5 μm metal-strip width [15], 450 nm core gap, LRSPP waveguide, resulting in η_{fiber} ~80%. The propagation losses, η_W and η_g, were determined by the FEM [14], and R_{Bragg} by the transfer matrix method [16]. Within a total loss of the 30 dB detection limit marked by the dashed line in Fig. 4(c), the grating length can be lengthened up to ~6 mm for a better resolution in thickness of the adsorption molecule layer. The thickness resolution of the adsorption layer shown in Fig. 4(d) is on the order of 0.1 nm for the grating length of 2 mm ~6 mm, and for the grating depth of 20 nm ~80 nm.

4. Conclusion

In summary, we have proposed a Bragg-grating resonance sensor based on LRSPP excitation on an asymmetric double-electrode waveguide structure. The asymmetric double-electrode LR-SPP Bragg grating biosensor with a sub-micron μ-fluidic channel has a bulk index resolution of 10^{-6} and a thickness detection limit of sub-nm, which are comparable with other waveguide based biosensors [5]. Use of the asymmetric double-electrode LRSPP waveguide structure has several merits. First, the symmetric requirement surrounding the metallic waveguide to sustain a LRSPP mode is inherently satisfied in the asymmetric double-electrode structure. While keeping symmetry in the media between the top and bottom claddings, the central thin slab dielectric core bounded by the two metal layers can be filled with any dielectric. The second merit comes from the low index guiding nature of the LRSPP modes. The material refractive index of the core (or channel fluid) is always lower than the cladding index while keeping the LRSPP mode index higher than the cladding by virtue of the double metal layers. This low-index core allows us to use a water-based buffer solution containing target molecules, or even gaseous biomolecules funneling through the μ-fluidic channel in a gas sensor chip. A unique advantage of the double-electrode LRSPP sensor is the versatility of signals carried by the double electrodes. A current or voltage signal can be applied to the electrodes while a LRSPP mode propagates on the same electrodes. This applied current (voltage) signal would generate heat (electrostatic force) to refresh the sensing surfaces, so the target analytes immobilized on the adsorption layer can be detached at any time for a new measurement.

The proposed LRSPP waveguide sensor utilizes spectral resonance of the asymmetric double-electrode structure by adding a Bragg grating in the core. It is possible to implement this asymmetric double-electrode structure in other sensor platforms based on interferometers, ring resonators, or microcavity photonic-crystals [5]. The sub-μm fluidic channel between the two metal layers is always under the highly confined LRSPP modes excited by end-fire coupling with optical fibers, therefore the proposed LRSPP sensor platform can be applied in a variety of integrated sensor-chip scenarios.

Acknowledgement

This work supported by the IT R&D program [2008-F-022-01] of the MKE/IITA, Korea and the Research fund of HYU (HYU-2008-T) and the Korea Science and Engineering Foundation(KOSEF) grant funded by the Korea government(MEST) [R01-2008-000-11852-02008] and the Seoul Science Fellowship.

#111165 - $15.00 USD Received 11 May 2009; revised 3 Jun 2009; accepted 3 Jun 2009; published 9 Jun 2009